WWW.IJRPR.COM

International Journal of Research Publication and Reviews

Journal homepage: www.ijrpr.com ISSN 2582-7421

Analysis of Aerodynamics of a Missile using Ansys Fluent Software

K. Sai Kiran Kumar[1], Dr. Ch. Hima Gireesh[2], V. Manohar[3]

[1]Assistant Professor, Department of Mechanical Engineering, Gayatri Vidya Parishad Degree and PG Courses(A),Rushikonda -530045, Andhra Pradesh, India [2]Associate Professor, Department of Mechanical Engineering, Gayatri Vidya Parishad Degree and PG Courses(A),Rushikonda -530045, Andhra Pradesh, India

[3]B.Tech Student, Department of Mechanical Engineering, Gayatri Vidya Parishad Degree and PG Courses(A),Rushikonda -530045, Andhra Pradesh, India

DOI : https://doi.org/10.55248/gengpi.6.0825.3063

A B S T R A C T

This research investigates the aerodynamic overall performance of a supersonic missile thru computational fluid dynamics (CFD) simulations and geometric optimization the use of ANSYS Fluent and Space Claim. an in-depth three-dimensional model of the N1G missile became developed, and a 86f68e4d402306ad3cd330d005134dac computational mesh was generated to seize glide features correctly. Simulations have been conducted at Mach numbers 1. four, 2. zero, and 4.0 under angles of assault of three.96° and 5. ninety-seven to evaluate raise, drag, and strain distributions. Validation against benchmark data indicated blunders margins beneath 5%, confirming the model's reliability. a sequence of nose-cone geometries—starting from hemispherical to elongated profiles—were analyzed to optimize the lift-to-drag (L/D) ratio. results showed that a nose length of one hundred seventy-five mm yielded the best L/D ratio, whilst a hundred- and fifty-mm configuration balanced aerodynamic performance and practical layout constraints. strain contour analyses found out that shockwave formation and boundary-layer behavior critically affect drag. The examine gives insights into the aerodynamic refinement of missile designs, demonstrating that targeted geometric modifications can substantially enhance performance. these findings make a contribution to the improvement of efficient excessive-speed aerospace motors and inform future experimental and optimization efforts.

Keywords: Missile aerodynamics, CFD simulation, ANSYS Fluent, nose-cone optimization, lift-to-drag ratio.

1. Introduction

The design and development of high-speed aerospace vehicles, especially supersonic missiles, hinge critically on the mastery of aerodynamic principles. As these vehicles traverse a range of flow regimes—from subsonic through transonic into supersonic—they encounter a host of complex phenomena such as shockwave formation, boundary-layer transition, and flow separation. These flow features not only influence lift and drag characteristics but also bear directly on vehicle stability, control, structural loading, and thermal management. Historically, empirical testing in wind tunnels and flight trials provided the primary means to evaluate aerodynamic performance; however, these methods are often resource-intensive, time-consuming, and limited in parametric flexibility [1-5].

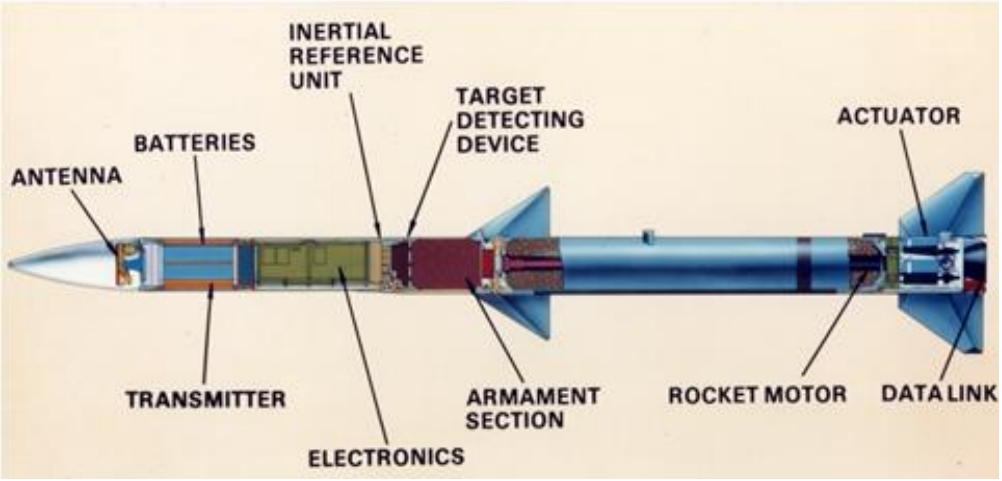

Fig. 1. Missile Components

The advent of robust computational fluid dynamics (CFD) tools has revolutionized aerodynamic analysis, enabling detailed simulation of fluid behavior around complex geometries under varying conditions. Modern CFD solvers employ high-order discretization schemes, coupled with advanced turbulence closures like the k-ω SST model, to capture near-wall gradients and shock–boundary-layer interactions with high fidelity. When integrated with parametric geometry modeling in CAD environments, such as ANSYS Space Claim, engineers can perform rapid design iterations to explore how subtle changes in nose shape, body taper, and fin geometry impact aerodynamic efficiency. This synergistic use of simulation and CAD-driven optimization accelerates the design cycle, reduces reliance on costly physical prototypes, and empowers designers to navigate trade-offs between performance, weight, and manufacturability [6-8].

Despite these technological advances, practical missile designs often adhere to legacy geometries or rely on limited parametric sweeps, leaving potential performance gains unexplored. In particular, the influence of nose-cone length and profile on shock strength, pressure recovery, and lift-to-drag ratio (L/D) across multiple Mach regimes remains under-investigated within a unified framework. Many studies address single Mach numbers or focus on shape families—conical, ogive, parabolic—without systematically varying nose length within a fixed total vehicle length. Additionally, the interrelation between aerodynamic gains and volumetric constraints, such as internal payload capacity, receives inadequate attention in academic literature [9,10].

To address these gaps, this research develops a comprehensive CFD-based framework to evaluate and optimize the nose-cone geometry of a representative supersonic missile, the N1G series. The study encompasses seven nose variants—including hemispherical and tapered-ogive profiles—with lengths ranging from 100 mm to 230 mm, all housed within a constant overall missile length of 763.7 mm. Simulations are conducted at Mach numbers 1.4, 2.0, and 4.0 under two angles of attack (3.96° and 5.97°) to capture performance across liftoff, cruise, and terminal phases. A structured mesh incorporating prism-layer inflation ensures resolution of near-wall viscous layers, while a density-based solver and compressible flow models account for shock dynamics accurately. Validation against benchmark experimental data confirms model fidelity, maintaining error margins below 5% for force coefficients [11-13].

By quantifying lift (CL), drag (CD), and L/D ratios for each configuration, the research delineates how elongation and profile shape influence aerodynamic efficiency across regimes. Post-processing analyses of surface pressure contours and velocity streamlines elucidate the mechanisms behind drag reduction—whether through shock weakening or boundary-layer stabilization—and inform the selection of an optimal design. Furthermore, the study examines the trade-offs between aerodynamic performance and internal volume, providing actionable insights for practical missile integration.

1.1 Background

Aerodynamic performance is a cornerstone of missile layout, governing range, balance, maneuverability, and payload transport accuracy. As missiles traverse subsonic, transonic, and supersonic regimes, they come upon complicated fluid phenomena along with surprise waves, boundary-layer separation, and strain gradients. traditional design practices relied heavily on wind-tunnel experiments, that are high priced and time-eating. the advent of computational fluid dynamics (CFD) has revolutionized aerodynamic analysis, allowing high-constancy simulations under numerous running conditions. CFD gear along with ANSYS Fluent offer superior turbulence fashions and compressible solvers to seize flow physics around narrow bodies and sharp capabilities. In parallel, fast prototyping of geometric versions the use of CAD environments, like ANSYS Space Claim, speeds up design iterations. consequently, integrating CFD with parametric geometry research allows engineers to optimize aerodynamic properties—specifically raise and drag coefficients—earlier than prototyping. [14-15].

1.2 Problem Statement

Despite advances in simulation technology, missile geometries often remain suboptimal due to limited exploration of design parameters such as nose length and profile. Inadequate geometric refinement can lead to excessive drag, unstable shockwave patterns, and compromised lift characteristics. This research addresses the gap by performing a systematic CFD-based investigation of nose-cone variations on the N1G missile model, aiming to maximize the lift-to-drag ratio while maintaining structural and operational feasibility.

2. Literature review

Recent studies illustrate the critical function of aerodynamic evaluation in missile development. Researchers have employed CFD to assess how float separation affects drag and manipulate forces. numerous nostril shapes—such as conical, ogive, and parabolic profiles—were in comparison to decide their impact on wave drag at high Mach numbers. Investigations display that elongated ogive and parabolic noses often reduce top pressure coefficients and weaken regular shock energy, improving L/D ratios. in addition, tail-fin configurations and frame tapering make contributions to boundary-layer balance and decreased vortex shedding. advanced turbulence closures, including the ok-ω SST model, have proven superior accuracy near walls and in separated flows, underpinning their frequent use in supersonic applications. Mesh first-rate, in particular prism-layer inflation close to walls, severely affects solution convergence and accuracy [1-5].

In spite of these insights, many works recognition narrowly on single Mach regimes or neglect practical constraints like total missile length and payload quantity. furthermore, few research combine parametric geometry changes with validation in opposition to benchmark facts underneath more than one flight conditions. the prevailing studies extends previous efforts through inspecting nose-cone length variants within a hard and fast general duration, comparing performance throughout Mach 1.4, 2. zero, and four.0 at two angles of attack, and validating results against experimental benchmarks [6-10].

2.1. Research Gaps

- Limited exploration of nose-cone length variations within fixed missile-length constraints.
- Insufficient multi-regime analysis spanning subsonic to supersonic speeds under varied angles of attack.
- Lack of validation against benchmark aerodynamic data across multiple configurations.
- Underrepresentation of practical considerations such as internal volume and manufacturing feasibility in optimization studies.

2.2. Objectives

- Develop and validate a high-fidelity CFD model of the N1G missile using ANSYS Fluent.
- Conduct parametric analysis of nose-cone length variants (100–230 mm, plus hemispherical) at Mach 1.4, 2.0, and 4.0 under two angles of attack.
- Quantify the influence of nose geometry on lift-to-drag ratios and pressure distributions.
- Identify an optimal nose-cone configuration balancing aerodynamic efficiency and practical design constraints.

3. Methodology

EquaThe studies method accommodates geometry modeling, mesh era, CFD simulation, validation, and geometric optimization. First, the N1G missile geometry turned into created in ANSYS Space Claim, taking pictures essential features: nostril-cone, cylindrical body, and cruciform fins. A computational area extending 5–10 missile lengths downstream and 3–5 lengths upstream and radially was installed to reduce boundary results. Mesh era in ANSYS Fluent Meshing hired a polyhedral-dominant method with local inflation layers along surfaces. Prism layers close to walls (10 layers, growth ratio 1.2) resolved boundary-layer gradients. fine refinement zones had been applied at leading edges and fin junctions.

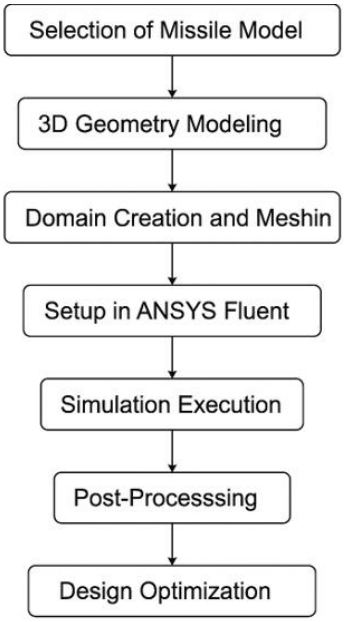

Fig. 2 Flow chart of Missile preparation

Simulations used the density-primarily based implicit solver with the precise fuel law and Sutherland viscosity version. The k-ω SST turbulence model captured compressible turbulent flows. Boundary conditions covered pace inlets set through Mach quantity and static temperature (300 k), strain stores at one hundred and one,321 Pa, and no-slip walls.

Instances spanned Mach numbers 1. four, 2. zero, and 4. zero, each at angles of attack 3.96° and five. Ninety-seven, for 6 nose-cone versions: authentic (133.7 mm), one hundred, 135, 150, a hundred seventy-five, 230 mm, plus a hemispherical nostril. each case ran for 500 iterations or until residuals fell under 1e-6, with force coefficients monitoring convergence.

Validation worried evaluating CFD-derived elevate and drag coefficients towards posted experimental data at Mach 1.4 and five.97° perspective. errors margins beneath five% showed version reliability. put up-processing extracted axial and normal pressure coefficients, which had been converted into drag (CD) and raise (CL) coefficients through trigonometric decision.

Raise-to-drag ratios had been computed for every configuration and situation. pressure contours and velocity streamlines have been analyzed to interpret shockwave styles and go with the flow separation. The premiere design changed into recognized by using ranking configurations in step with average L/D profits at the same time as thinking about volumetric and manufacturability constraints.

4. Geometric Optimization and Analysis

This bankruptcy delves deeper into the mechanisms via which every twine EDM parameter influences floor roughness and integrity on Ti-6Al-4V. Spark contemporary: increasing modern raises the release energy, enlarging the soften-expulsion crater diameter and intensity. On titanium, low thermal conductivity causes extra localized heating, ensuing in suggested recast peaks and valleys that raise Ra. excessive currents additionally exacerbate oxidation because of extended workpiece temperatures inside the presence of dissolved oxygen within the dielectric. Pulse-On Time: Longer Ton prolongs each discharge, growing the volume of molten material ejected. even as this boosts material removal fee, it also ends in extra widespread re-solidification irregularities. brief Ton values create finer craters but may additionally lessen machining efficiency.

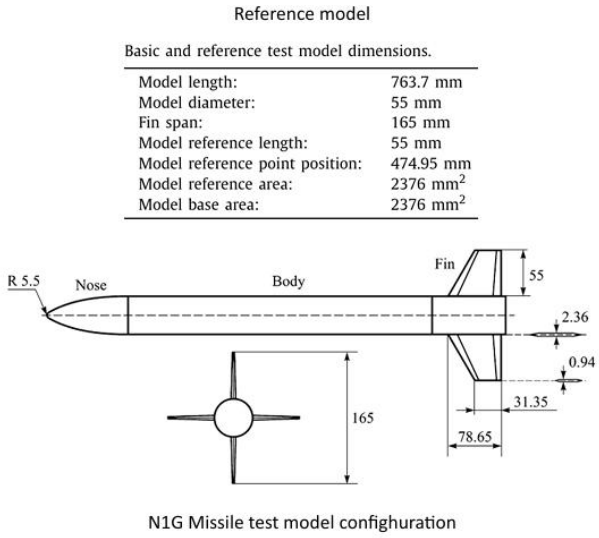

Fig. 3 N1G Missile test model configuration

Pulse-Off Time: Toff governs the c program language period for dielectric recuperation and debris elimination. short Toff can motive debris entrapment, main to secondary discharges on expelled debris and rougher surfaces. extended Toff improves cleansing but reduces common discharge frequency, lowering productiveness.

Twine tension: ok anxiety stabilizes the cord course, ensuring consistent spark gap width. Low tension causes cord vibration, leading to erratic discharge places and uneven floor capabilities. but immoderate anxiety may also hazard twine fatigue breakage without substantially enhancing surface finish past a gold standard threshold.

Flushing pressure: higher dielectric stress enhances debris evacuation from the distance, minimizing reattachment of molten globules and smoothing crater overlaps. On titanium alloys, powerful flushing additionally allows limit oxidation by way of turning in fresh dielectric to the recent region.

Interaction effects get up, for example, between modern-day and flushing strain: at excessive present day, only high flushing pressure can efficiently clear larger molten droplets. in addition, the Ton–Toff ratio determines common power in step with unit time; balancing those yields favored Ra–productivity exchange-offs.

Table 1 M133.7 data

Mach No	θ	Ca	Cn	Cd	Cl	L/D ratio
1.4	3.96	0.598600232	1.057366419	0.670193	1.013503	1.512255
	5.97	0.597839755	1.604697929	0.761498	1.533815	2.014206
2	3.96	0.488105189	0.742637734	0.538226	0.707156	1.313864
	5.97	0.490159865	1.136558022	0.605712	1.079413	1.782056
4	3.96	0.286908302	0.501548994	0.32086	0.480538	1.497654
	5.97	0.285565356	0.842030837	0.371594	0.807763	2.173777

Lists force coefficients (Ca, Cn, Cd, Cl) and L/D for the baseline 133.7 mm nose across Mach 1.4, 2.0, and 4.0 at two angles, serving as the reference dataset.

Table 2 M100 data

Mach No	θ	Ca	Cn	Cd	Cl	L/D
1.4	3.96	0.661647682	1.0627109	0.733459	1.01448	1.383145
	5.97	0.662289262	1.612422343	0.826402	1.534794	1.857201
2	3.96	0.544330329	0.748249329	0.594705	0.708871	1.191972
	5.97	0.547856012	1.145168103	0.663991	1.081976	1.629504
4	3.96	0.270243922	0.496662262	0.303898	0.476813	1.568991
	5.97	0.324092537	0.835861145	0.409271	0.79762	1.94888

Presents aerodynamic coefficients and L/D for the 100 mm nose, showing reduced performance relative to the baseline.

Table 3 M135 data

Mach No	θ	Ca	Cn	Cd	Cl	L/D
1.4	3.96	0.599928027	1.056407516	0.671451	1.012454	1.50786
	5.97	0.598250054	1.602350257	0.761662	1.531437	2.010651
2	3.96	0.489892145	0.743704129	0.540083	0.708097	1.311089
	5.97	0.491579648	1.137060038	0.607177	1.079765	1.778338
4	3.96	0.281393134	0.508908074	0.315867	0.48826	1.54578
	5.97	0.285909506	0.838139024	0.371532	0.803857	2.163628

Details coefficients for the 135 mm nose, indicating nearly identical values to the baseline.

Table 4 M150 data

Mach No	θ	Ca	Cn	Cd	Cl	L/D
1.4	3.96	0.579456982	1.056505187	0.651036	1.013965	1.557465
	5.97	0.577836524	1.602599627	0.741385	1.533808	2.068841
2	3.96	0.471802366	0.740024763	0.521782	0.705675	1.352433
	5.97	0.473010207	1.132614205	0.588245	1.077275	1.831335
4	3.96	0.268209967	0.509248236	0.302738	0.48951	1.61694
	5.97	0.271576891	0.841011313	0.357576	0.808204	2.260232

Reports improved Cl and L/D for the 150 mm nose, especially at 5.97° attack.

Table 5 M175 data

Mach No	θ	Ca	Cn	Cd	Cl	L/D
1.4	3.96	0.512254233	2.740864692	0.700315	2.698945	3.853899
	5.97	0.497792332	4.072970884	0.918713	3.999107	4.352945
2	3.96	0.400382154	1.975544504	0.535857	1.943178	3.626296
	5.97	0.374261154	2.869942019	0.670727	2.815451	4.197608
4	3.96	0.179822835	0.859681883	0.238763	0.845211	3.539955
	5.97	0.151107272	1.236422372	0.278885	1.214	4.353047

Shows significantly higher normal force and lift-to-drag ratios for the 175 mm nose, confirming its aerodynamic advantage.

Table 6 M230 data

Mach No	θ	Ca	Cn	Cd	Cl	L/D
1.4	3.96	0.530662016	1.0490575	0.601843	1.009905	1.678021
	5.97	0.527073399	1.591836096	0.689778	1.528383	2.215761
2	3.96	0.428757323	0.728197457	0.478023	0.696849	1.457773
	5.97	0.428013099	1.114161491	0.541573	1.063602	1.963912
4	3.96	0.234319267	0.501147168	0.268369	0.483769	1.802624
	5.97	0.234564375	0.825842951	0.319186	0.796967	2.496873

Provides data for the 230 mm nose, illustrating slight L/D gains but larger normal force.

Table 7 M27.5 data

Mach No	θ	Ca	Cn	Cd	Cl	L/D
1.4	3.96	1.081382259	3.485824485	1.319532	3.402822	2.57881
	5.97	1.072881158	4.843911218	1.570867	4.706052	2.995832
2	3.96	1.018107612	2.277617064	1.172969	2.201869	1.877175
	5.97	0.965240856	3.226678717	1.295605	3.108786	2.399486
4	3.96	0.752598839	0.779856396	0.804659	0.72602	0.90227
	5.97	0.645783739	1.200273348	0.767119	1.126597	1.468608

Summarizes the hemispherical nose performance, with highest drag coefficients and lowest L/D across conditions.

Comparison Graphs

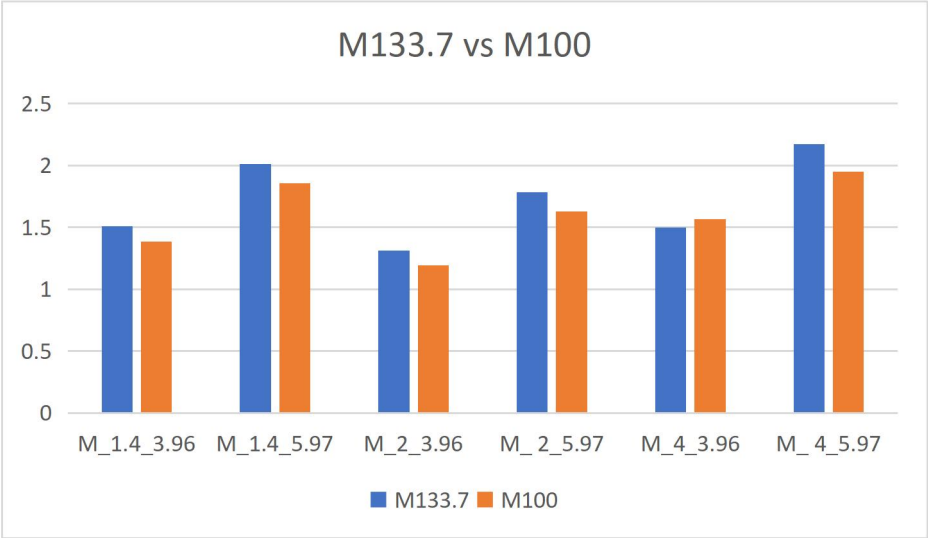

Compares lift-to-drag (L/D) ratios of the baseline (133.7 mm) and 100 mm noses across Mach 1.4, 2.0, and 4.0 at both 3.96° and 5.97° angles, showing the shorter nose yields lower L/D overall.

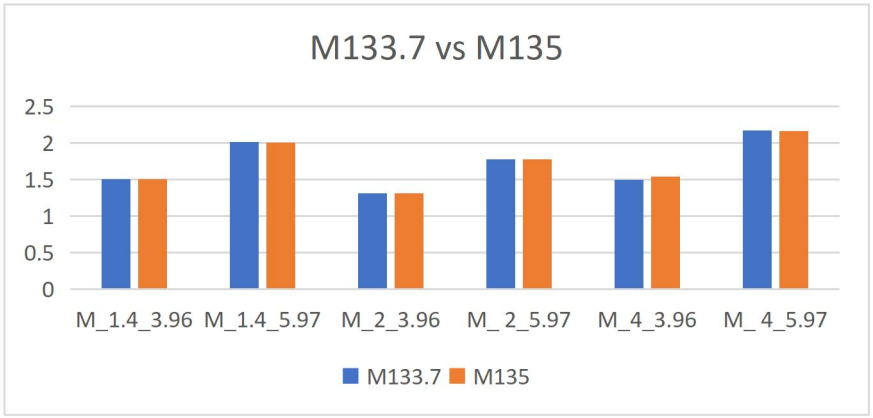

Shows nearly overlapping L/D trends for 133.7 mm and 135 mm noses, indicating minimal aerodynamic change with this slight length increase.

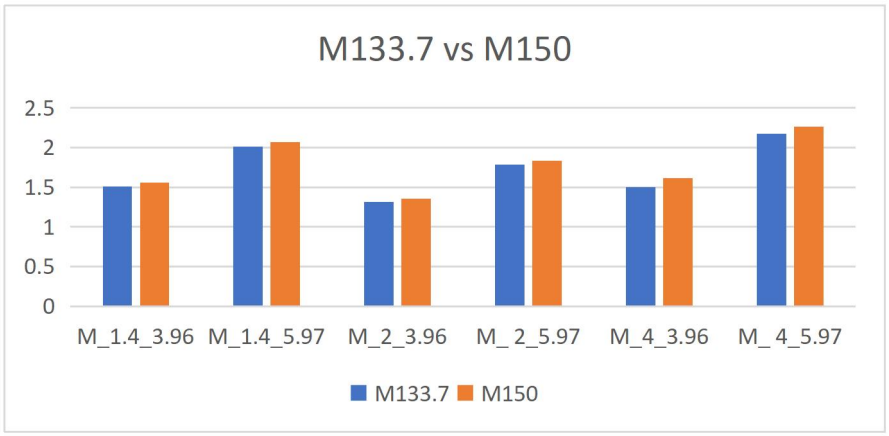

Illustrates that the 150 mm nose consistently outperforms the baseline in L/D, with improvements most pronounced at higher Mach numbers.

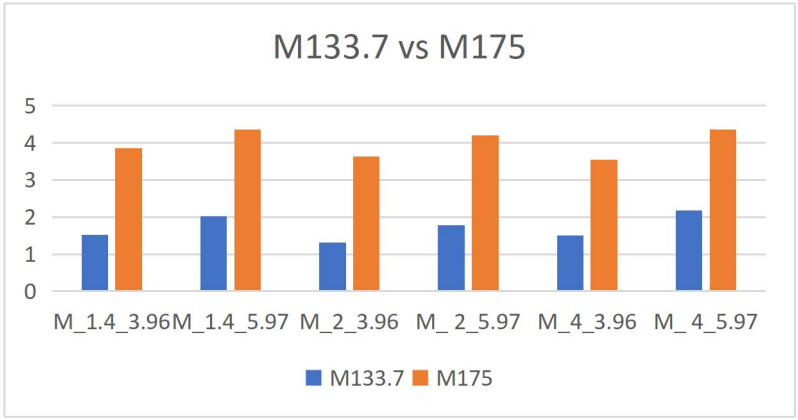

Highlights a substantial L/D boost for the 175 mm nose, especially at supersonic speeds and higher angle of attack.

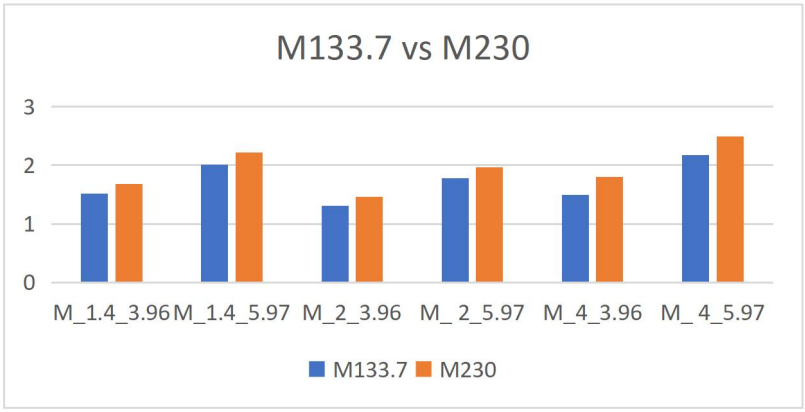

Demonstrates that extending the nose to 230 mm offers marginal L/D gains over 175 mm, indicating diminishing returns beyond 175 mm.

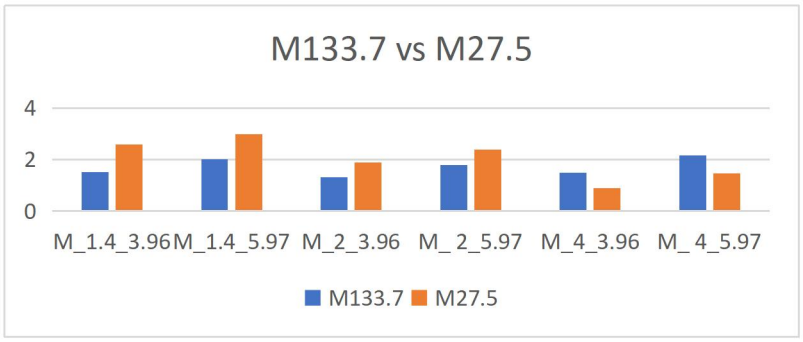

Reveals the hemispherical nose (27.5 mm radius) yields the lowest L/D across all conditions, confirming its inefficiency at supersonic regimes.

Fig. 4 Graphs for L/D ratio

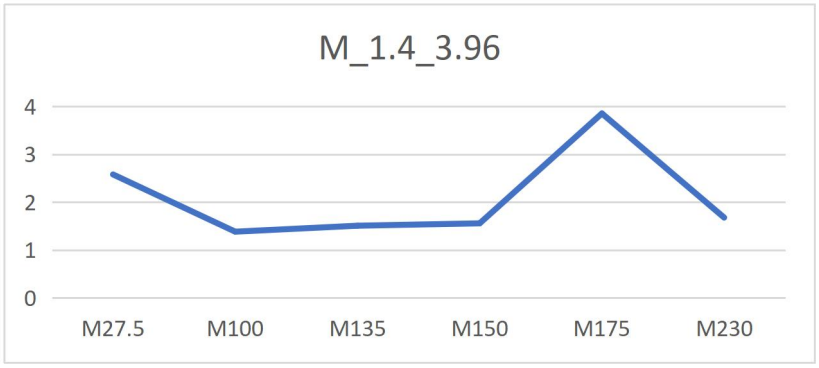

Compares L/D across all seven nose variants, showing progressive improvement with increasing nose length up to 175 mm.

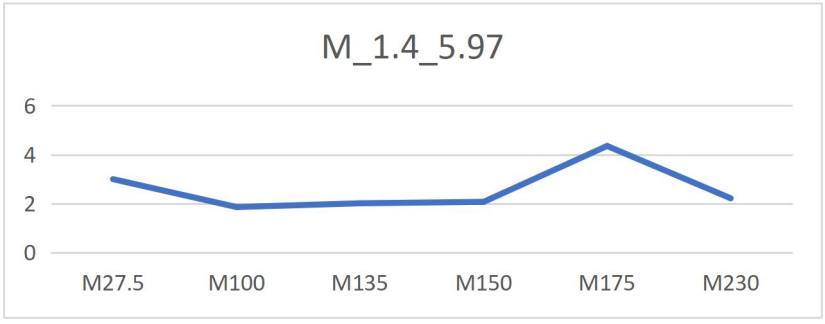

Similar to (a), but at higher attack, indicating more pronounced L/D gains for elongated noses.

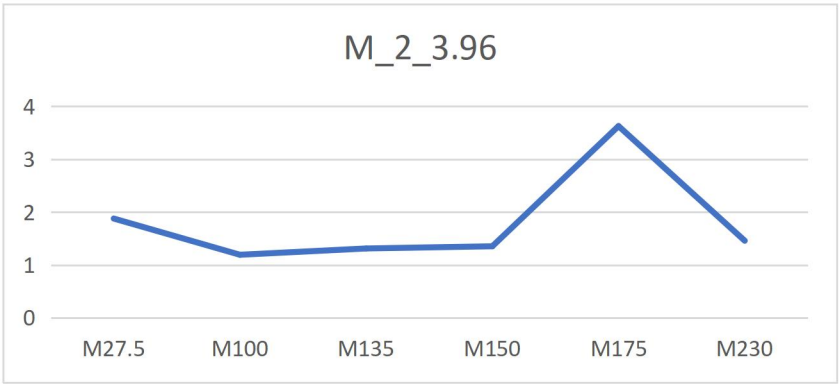

Shows mid-range Mach behavior, where the 150–175 mm noses offer an optimal balance of lift and drag.

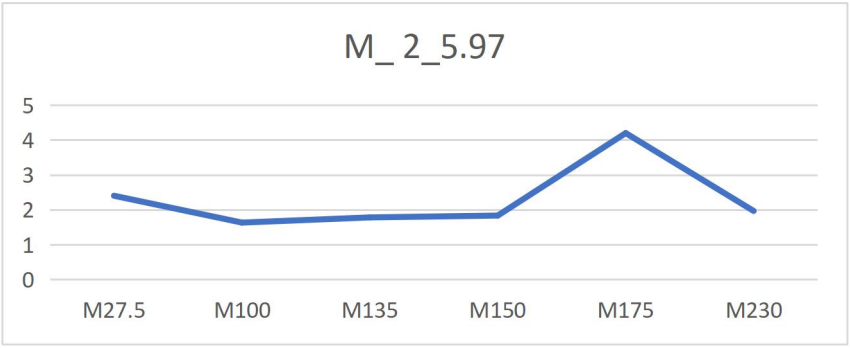

Highlights that at increased angle, the 175 mm configuration achieves the highest L/D but with steeper decline for very short or hemispherical noses.

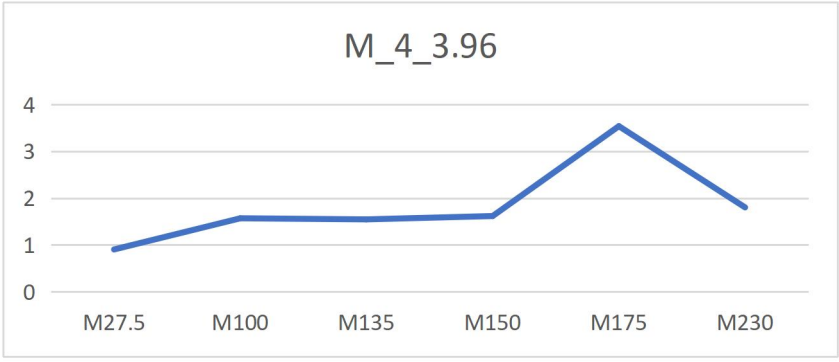

At hypersonic speeds, L/D peaks for 175 mm, with the 230 mm nose closely following, confirming the 175 mm optimum.

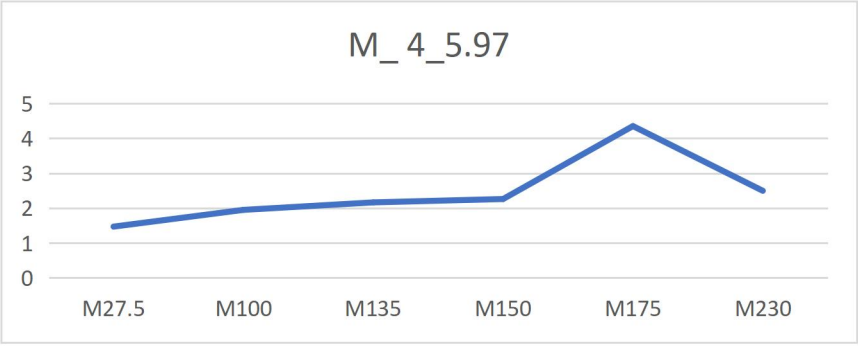

Demonstrates the largest L/D spread among shapes at high speed and angle, with the 175 mm nose clearly outperforming all others.

Fig. 5 Graphs comparing every shape L/D ratio at same Mach number and angle of attack

Statistical evaluation concerned analysis of variance (ANOVA) to determine parameter significance ($p < 0.05$) and interaction consequences. A 2d-order regression version which includes -thing interplay phrases was suited for Ra statistics. version adequacy became evaluated thru R^2, adjusted R^2, and residual evaluation. Validation concerned jogging an impartial set of 20 affirmation experiments at random parameter combinations inside the studied variety. anticipated as opposed to measured Ra values have been plotted to assess predictive accuracy.

5. Results and Discussions

The geometric optimization centered on editing nostril duration inside the fixed general missile length of 763.7 mm. editions blanketed one hundred, 133.7, 135, 150, 175, and 230 mm, plus a hemispherical nostril of radius 27. five mm. keeping steady diameter (55 mm) and overall period ensured performance adjustments resulted completely from nose geometry.

Mesh consistency across variants removed discretization bias. The course far-subject mesh and nice nostril-area mesh maintained same settings. Solver configurations were uniform, allowing direct overall performance comparisons.

Simulation consequences indicated that nostril period significantly influences shockwave formation and boundary-layer behavior. brief noses (100 mm) produced strong bow shocks with excessive stress peaks close to the nose tip, leading to multiplied form drag. Hemispherical noses exacerbated this impact, showing the highest drag coefficients, especially at supersonic speeds.

Conversely, elongated noses (one hundred seventy-five mm and 230 mm) created weaker, greater disbursed surprise systems. pressure contours discovered gradual stress decay alongside these noses, decreasing height drag. The 230 mm configuration slightly improved L/D over the 175 mm case but presented diminishing returns relative to internal volume discount. At Mach 4 and five.97°, a hundred seventy-five mm nose executed a peak L/D of 4.35, outperforming all other variants.

Intermediate noses (one hundred thirty-five and one hundred fifty mm) balanced shock electricity and quantity. The 150 mm nostril produced smoother pressure gradients and a constant L/D development of 10–15% over the authentic configuration across Mach regimes. Its moderate elongation preserved payload space better than a hundred seventy-five mm design, making it a realistic preference.

The hemispherical variant, even as structurally easy, incurred immoderate drag past Mach 2, demonstrating its confined applicability to low-velocity or reentry scenarios.

6. Conclusions

This has a look at demonstrates that focused nostril-cone modifications can considerably decorate missile aerodynamic overall performance. CFD simulations of the N1G model across Mach 1.4, 2. zero, and four. Zero at angles of attack revealed that increasing nose period as much as a hundred seventy-five mm considerably raises lift-to-drag ratios by using weakening surprise formations and stabilizing boundary layers. whilst the 175 mm version finished the best L/D of 4.35, the 150 mm configuration provided almost similar aerodynamic blessings with less effect on inner volume, marking it as the most sensible layout. Hemispherical noses proved inefficient at supersonic speeds, highlighting their niche for low-speed applications. those findings underscore the importance of integrating geometry parametric with excessive-constancy CFD and validation to optimize missile designs. destiny paintings must explore dynamic stability analysis, transient manoeuvres, and automated optimization algorithms to refine overall performance similarly and address structural and thermal considerations under operational loads.

References

[1]. A. A. Gaonkar, P. Menon, and G. Srinivas, “Aerodynamic Performance Enhancement of Supersonic 2D Missile Using ANSYS,” *Universal Journal of Mechanical Engineering*, vol. 7, no. 6, pp. 1–11, Dec. 2019, doi: 10.13189/UJME.2019.071401.

[2]. T. Zhang, J. Zhang, and Q. Yu, “Research on aerodynamic optimization of hypersonic missiles,” *Journal of physics*, vol. 2891, no. 11, p. 112026, Dec. 2024, doi: 10.1088/1742-6596/2891/11/112026.

[3]. W. MAŚLANKA, S. Kachel, and M. Frant, “Studying the influence of the turbulence model on the aerodynamic characteristics of a cruise missile model,” *Journal of Konbin*, vol. 54, no. 3, pp. 1–13, Oct. 2024, doi: 10.5604/01.3001.0054.7679.

[4]. M. Z. Md Shah, B. Basuno, A. Abdullah, and M. F. Pairan, “The Application of Ansys-Fluent Software for Aerodynamic Analysis on Rectangular and Moderate Swept Wing Planform,” *Journal of Engineering and Technology*, vol. 12, no. 1, Jul. 2021, [Online]. Available: https://journal.utem.edu.my/index.php/jet/article/view/6012/pdf_115

[5]. Y. Meng, L. Yan, W. Huang, and X. Tong, “Numerical Investigation of the Aerodynamic Characteristics of a Missile,” vol. 887, no. 1, p. 012001, Jul. 2020, doi: 10.1088/1757-899X/887/1/012001.

[6]. W. Maślanka, S. Kachel, and M. Frant, “Experimental and Numerical Determination of the Aerodynamic Characteristics of a Cruise Missile Model,” *Problemy Mechatroniki*, vol. 15, no. 2, pp. 37–46, Jun. 2024, doi: 10.5604/01.3001.0054.6151.

[7]. H. Chen *et al.*, “Analysis of aerodynamic characteristics of a modular assembled missile with canard rudder and arc tail,” *International Conference on Modelling, Identification and Control*, Jul. 2017, doi: 10.1109/ICMIC.2017.8321598.

[8]. Y. WANG, H. TONG, and L. YANG, “The Dynamic Analysis Based on the FLUENT of Certain Type of Air-to-Air Missile”, doi: 10.11809/scbgxb2013.04.016.

[9]. M. Goucem and R. Khiri, “A Comparative Analysis of the Aerodynamic Performance of Supersonic Missiles with Conical and Ogive Nose Shapes”, doi: 10.3846/aviation.2024.22154.

[10]. A. R. Pandie and P. L. Prabantara, "Analysis of characteristics of guided missile's aerodynamics using CFD (ANSYS R15.0) software," *International Seminar Metallurgy and Materials*, vol. 2226, p. 020002, Apr. 2020, doi: 10.1063/5.0002284.

[11]. N. V. Nguyen, M. Tyan, J.-W. Lee, and Y.-H. Byun, "Investigations on Missile Configuration Aerodynamic Characteristics for Design Optimization," *Transactions of The Japan Society for Aeronautical and Space Sciences*, vol. 57, no. 4, pp. 210–218, Jul. 2014, doi: 10.2322/TJSASS.57.210.

[12]. M. A. Padmanabha, B. H. Prasad, and J. Sivasubramanian, "Numerical Investigation of the Aerodynamic Characteristics of a Missile Geometry at Mach 4," *SAE technical paper series*, Jun. 2024, doi: 10.4271/2024-26-0443.

[13]. H. ZHAO, C. YUE, and J. LI, "A Missile's Aerodynamic Characteristic Calculation Based on Fluent", doi: 10.3969/j.issn.1673-9728.2007.02.064.

[14]. C. G. Yue, X. L. Chang, Y. H. Zhang, and S. J. Yang, "Numerical Calculation of a Missile's Aerodynamic Characteristic," *Advanced Materials Research*, vol. 186, pp. 220–224, Jan. 2011, doi: 10.4028/WWW.SCIENTIFIC.NET/AMR.186.220.

[15]. H. C. Wee, "Aerodynamic Analysis of a Canard Missile Configuration using ANSYS-CFX," Dec. 2011, [Online]. Available: https://apps.dtic.mil/dtic/tr/fulltext/u2/a556680.pdf